Modeling of Kinetics of Isothermal Idiomorphic Ferrite Formation in a Medium-Carbon Vanadium-Titanium Microalloyed Steel

C. CAPDEVILA, F.G. CABALLERO, and C. GARCÍA DE ANDRÉS

The present article is concerned with the theoretical and experimental study of the growth kinetics of idiomorphic ferrite in a medium-carbon vanadium-titanium microalloyed steel. A theoretical model is presented to calculate the evolution of isothermal austenite-to-idiomorphic ferrite transformation with time for a given temperature. Moreover, the nature, size, and distribution of the inclusions that are responsible for the intragranular nucleation of idiomorphic ferrite have been characterized by scanning electron microscopy (SEM). Finally, the influence of austenite grain size in the isothermal decomposition of austenite in idiomorphic ferrite has been thoroughly analyzed. An excellent agreement (higher than 90 pct in R^2) has been obtained between the experimental and predicted values of the volume fraction of idiomorphic ferrite.

I. INTRODUCTION

TOUGHNESS and other mechanical properties of steels are critically affected by their microstructure. It is well known that proeutectoid ferrite can nucleate at inclusions within coarse austenite grains, resulting in a very fine microstructure. Recently, this phenomenon has received great attention because of the need for toughness, especially when conventional austenite grain-refinement techniques are not enough.

Idiomorphic and acicular ferrite are the microstructures that affect the strength and, in particular, the toughness of weld deposits.[1–4] There is a large amount of work on acicular ferrite formation,[5–8] but, in contrast, idiomorphic ferrite formation has rarely been studied. Some studies reported that idiomorphs nucleate at precipitates of titanium oxide (Ti_2O_3), manganese sulfide (MnS), and vanadium nitride (VN).[1,9,10] Those studies also analyzed the reason such precipitates act as viable sites for intragranular ferrite nucleation. However, the nucleation and growth kinetics for idiomorphic ferrite formation were not investigated.

Although the kinetics of allotriomorphic ferrite,[11,12] pearlite,[13,14] and acicular ferrite formation are well established,[15] a kinetic theory for idiomorphic ferrite formation has not been adequately developed yet. This work aims to study the isothermal decomposition of austenite into idiomorphic ferrite and to analyze the influence of the prior austenite grain size (PAGS) on the nuleation and growth of idiomorphic ferrite. A mathematical model that describes the kinetics of idiomorphic ferrite formation during the isothermal decomposition of austenite is also proposed.

C. CAPDEVILA and F.G. CABALLERO, Research Associates, and C. GARCÍA DE ANDRÉS, Research Scientist, are with the Department of Physical Metallurgy, Centro Nacional de Investigaciones Metalúrgicas (CENIM-CSIC), E-28040 Madrid, Spain.

Manuscript submitted December 1, 2000.

II. EXPERIMENTAL

The chemical composition of the steel studied is presented in Table I. The material was supplied in the form of 50-mm-square bars, obtained by conventional casting as a square ingot (2500 kg) and hot rolling to bar.

The isothermal decomposition of austenite has been analyzed by means of a high-resolution dilatometer DT 1000 Adamel-Lhomargy described elsewhere.[16] Cylindrical dilatometric samples, 2 mm in diameter and 12 mm in length and machined parallel to the rolling direction of the bar, were used for these tests. The change in length of the specimen is transmitted *via* an amorphous silica push rod. This variation is measured by a linear variable differential transformer (LVDT) sensor in a gas-tight enclosure enabling testing under vacuum or an inert atmosphere with accuracy better than 0.1 μm. The dilatometric curve (relative change in length (dL/L_o) *vs* time (t)) is monitored with the help of a computer-assisted electronic device. The dilatometer is equipped with a very low thermal inertia radiation furnace. The heat radiated by two tungsten filament lamps is focused on the specimen by means of a bi-elliptical reflector. The temperature is measured with a 0.1-mm-diameter chromel-alumel (type K) thermocouple (Hoskins Mfg. Co., Michigan, USA) welded to the specimen. Cooling is carried out by blowing a jet of helium gas directly onto the specimen surface. The helium flow rate during cooling is controlled by a proportional servovalve. The heating and cooling devices of this dilatometer ensure an excellent efficiency in controlling both the temperature and the holding time of isothermal treatments, and the fast cooling in quenching processes.

With the aim of studying the influence of PAGS on the isothermal austenite-to-idiomorphic ferrite transformation, specimens were austenitized at two different temperatures (1273 and 1523 K) for 1 min. Subsequently, specimens were isothermally transformed at 913 K during different times and quenched under a helium gas flow at a cooling rate of 200 K/s. Specimens were ground and polished using standardized metallographic techniques, and subsequently etched with 2 pct Nital solution to reveal the ferrite microstructure through optical microscopy.

Table I. Chemical Composition (Weight Percent)

C	Si	Mn	Cr	Al	Ti	V	Cu	O	Mo	S
0.37	0.56	1.45	0.04	0.024	0.015	0.11	0.14	0.004	0.025	0.043

Table II. Prior Austenite Grain Size

T_γ, K	PAGS, μm
1523	76
1273	11

T_γ = austenitization temperature.

The PAGS measurements were made on micrographs. The average grain size was calculated using a linear intercept technique involving at least 50 intercepts, which made it possible to count the number of grains intercepted by the grid line. The effects of a moderately nonequiaxed structure were eliminated by counting the intersections of lines in four or more orientations covering all the observation fields with an approximately equal weight.[17] Table II shows the average PAGS in microns corresponding to both austenitization conditions.

Measurements of volume fraction of idiomorphic ferrite (V_{IDI}) were performed statistically by means of a systematic manual point counting procedure.[17] A grid superimposed on recorded micrographs provides, after a suitable number of placements, an unbiased statistical estimation of the V_{IDI}.

Finally, the morphology and nature of the inclusions were determined by means of scanning electron microscopy (SEM). Specimens were sectionalized longitudinally and transversally to the rolling direction, polished in the usual way, and finished with 0.5-μm diamond paste. Samples were slightly etched in a 2 pct Nital solution for SEM examination in a JEOL* JXA 840 scanning electron microscope operating at 15 kV with an energy dispersive X-ray (EDX) analysis unit. Quantitative information on the size distribution of inclusions was obtained by means of an IBAS OPTIMAS (Meyer Instruments, Houston, TX) 2.0 automatic image analyzer. The SEM images were digitized with a resolution of 512×512 pixels and with 256 gray levels. After the images enhancement processes, the size of the inclusions was determined through the measurement of the two perpendicular diameters in the transversal section (d_1 and d_2), and the highest diameter in the longitudinal section (d_3). For that propose, a 512×512-points grid was used along with magnifications as high as 3000 times to characterize inclusions with a diameter lower than 0.1 μm. A minimum of 500 particles was counted in each diameter to obtain a reliable result.

*JEOL is a trademark of Japan Electron Optics Ltd., Tokyo.

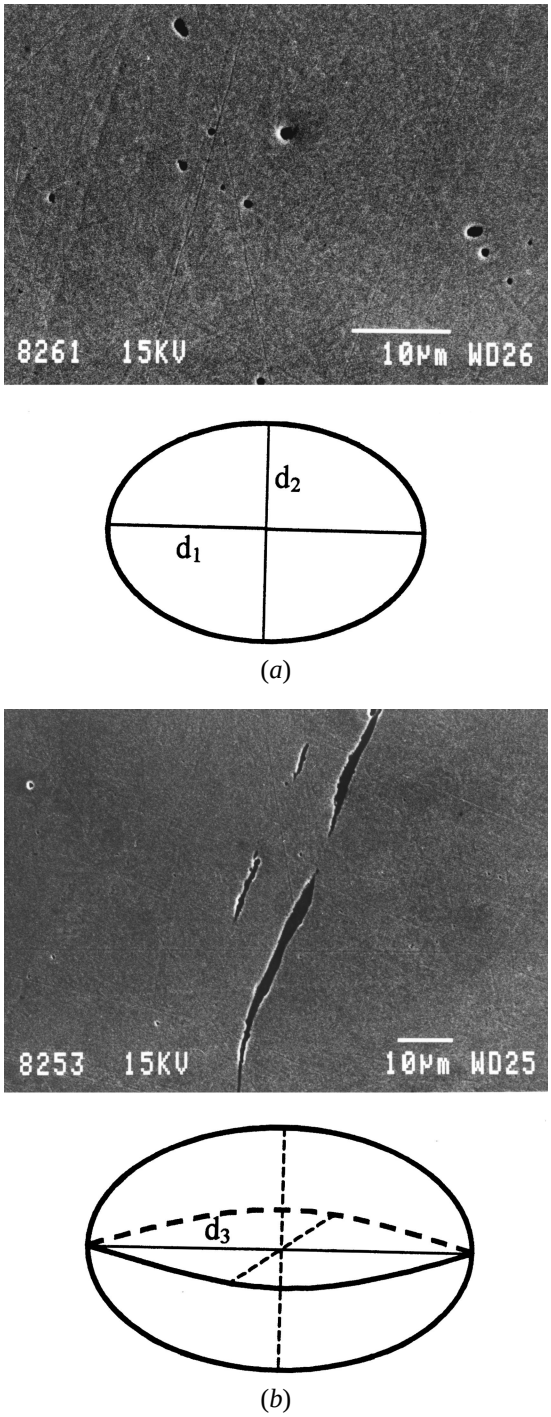

Fig. 1—Morphology of inclusions: (*a*) transverse and (*b*) longitudinal section to rolling direction.

III RESULTS AND DISCUSSION

A. *Size Distribution and Nature of Inclusions*

Figure 1 shows both the morphology of the inclusions in samples sectionalized longitudinally and transversally to the rolling direction, and a schematic illustration of their ellipsoidal shape. Figure 2 shows the frequency of the inclusion diameters experimentally obtained in a transversal (d_1 and d_2) and longitudinal (d_3) section. From the histograms of this figure, the average values of d_1, d_2, and d_3 have been obtained (Table III). The EDX spectrum in Figure 3 shows that all these inclusions are MnS.

Idiomorphic ferrite nucleates intragranularly in the inclusions distributed inside the austenite grains. Thus, the volume fraction of idiomorphic ferrite is related to the volume fraction of inclusions in the steel. Kluken and Grong[18] proposed an equation to estimate the volume fraction of inclusions by converting the analytical oxygen and sulfur

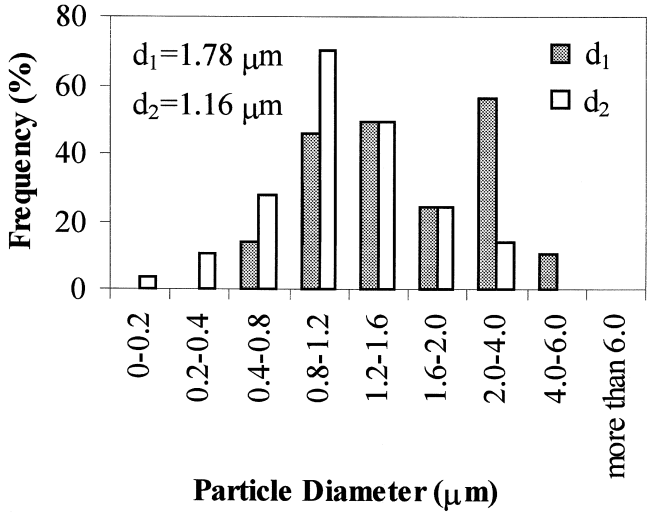

(*a*)

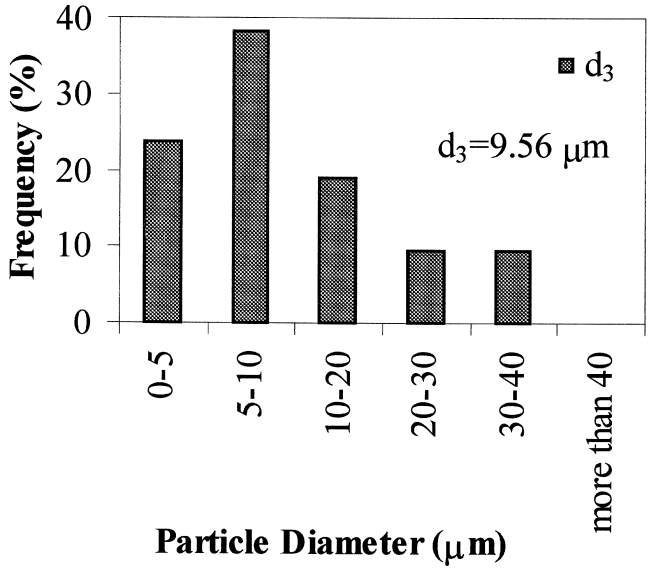

(*b*)

Fig. 2—Size distribution of inclusion: (*a*) transverse and (*b*) longitudinal section to rolling direction.

concentration in the steel into an equivalent inclusion volume fraction. Considering the solubility of sulfur in the steel equal to 0.003 wt pct,[19] the following equation has been derived:

$$V_V \approx 10^{-2}\,[5.0\{\text{pct O}\} + 5.4\,(\{\text{pct S}\} - 0.003)] \quad [1]$$

where V_V is the volume fraction of inclusions in the steel and O and S are the oxygen and sulfur concentration of the steel, respectively, in wt pct. For the studied steel, $V_V = 2.34 \times 10^{-3}$ (Table I shows the oxygen and sulfur composition).

B. *Role of PAGS in Idiomorphic Ferrite Formation*

Ferrite, which grows by diffusional mechanisms, can be classified into two main forms: allotriomorphic ferrite and idiomorphic ferrite.[20,21] Allotriomorphic ferrite nucleates at the prior austenite grain boundaries and tends to grow along the austenite boundaries at a rate faster than in the normal direction to the boundary plane (Figure 4). By contrast, idiomorphic ferrite nucleates at the inclusions inside the austenite grains and can be identified in the microstructure by its equiaxed morphology (Figure 4). Consequently, the balance between the number of intragranular nucleation sites and the number of sites at the austenite grain boundaries is a very important factor in the competitive process of allotriomorphic-idiomorphic ferrite formation.

Table III. Diameters of Ellipsoidal Inclusions

Transversal Section		Longitudinal Section
d_1, μm	d_2, μm	d_3, μm
1.78 ± 0.30	1.16 ± 0.20	9.56 ± 2.30

It is well known that an increase in the PAGS leads to a reduction in the number of nucleation sites at the austenite grain boundaries. Therefore, an increase in the PAGS indirectly favors the intragranular nucleation of ferrite: then, the formation of idiomorphic ferrite, rather than allotriomorphic ferrite, is enhanced. Likewise, as the PAGS increases, the number of inclusions trapped inside the austenite grains increases, which promotes the intragranular nucleation of ferrite.

Assuming that ferrite nucleates primarily on grain boundaries, Grong[22] reported that the total number of grain boundary nucleation sites per unit volume N_V^{GB} is given as

$$N_V^{GB} = n_a S_V^{GB} \quad [2]$$

where n_a is the number of nucleation sites per unit grain boundary area and S_V^{GB} is the grain boundary surface area per unit volume. The value of n_a can be expressed as K/δ^2 where K is a constant and δ is the atomic spacing (reasonable value of 2.5×10^{-10} m).[23] As a second approximation, it could also be assumed that the austenite grains are spherical in shape. Then, S_V^{GB} is given as

$$S_V^{GB} = \frac{\pi (d_\gamma/2)^2}{\frac{4\pi}{3}(d_\gamma/2)^3} = \frac{6}{d_\gamma} \quad [3]$$

where $d\gamma$ is the mean austenite grain diameter. In this work, a similar expression for the intragranular nucleation sites is proposed. Bearing in mind that n^{INC} is the total number of inclusions inside the austenite grain, the total inclusion surface area per unit volume S_V^{INC} could be expressed by

$$S_V^{\text{INC}} = S_{Vo}^{\text{INC}}\, n^{\text{INC}} \quad [4]$$

where S_{Vo}^{INC} is the inclusion surface area per unit volume for a particular inclusion. In this sense, and considering that all the inclusions are ellipsoids with the same size (average values are shown in Table III), S_{Vo}^{INC} is written as

$$S_{Vo}^{\text{INC}} = 6/d_3 \quad [5]$$

Moreover, n^{INC} could be expressed as the volume fraction of inclusions in the steel (V_V) modulated by the ratio between the austenite grain size and the inclusion size:

$$n^{\text{INC}} = \frac{d_\gamma}{(d_1 + d_2)/2}\, V_V \quad [6]$$

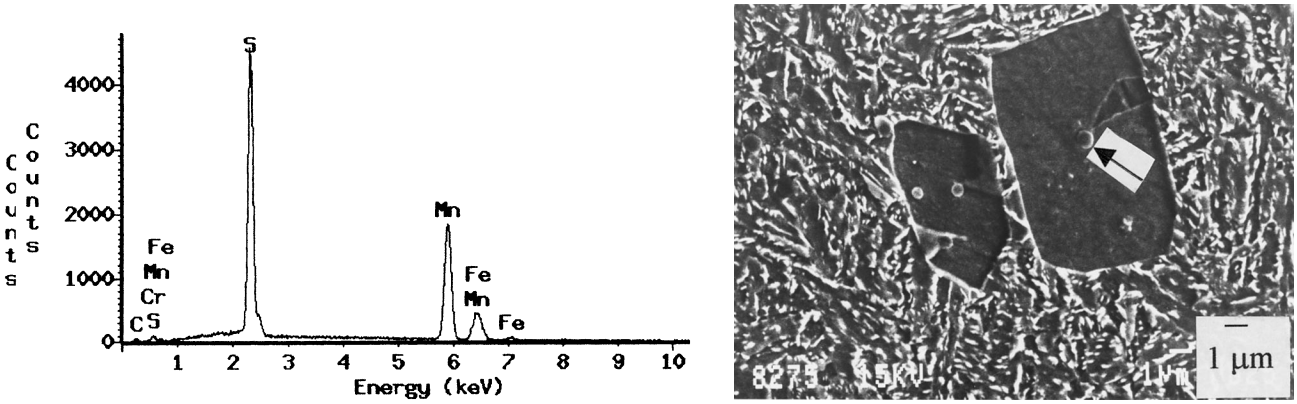

Fig. 3—EDX spectrum of an inclusion (arrow) where idiomorphic ferrite nucleates.

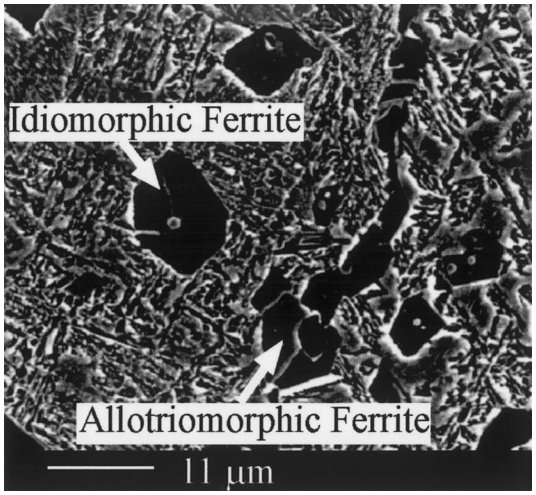

Fig. 4—SEM micrograph of idiomorphic and allotriomorphic ferrite.

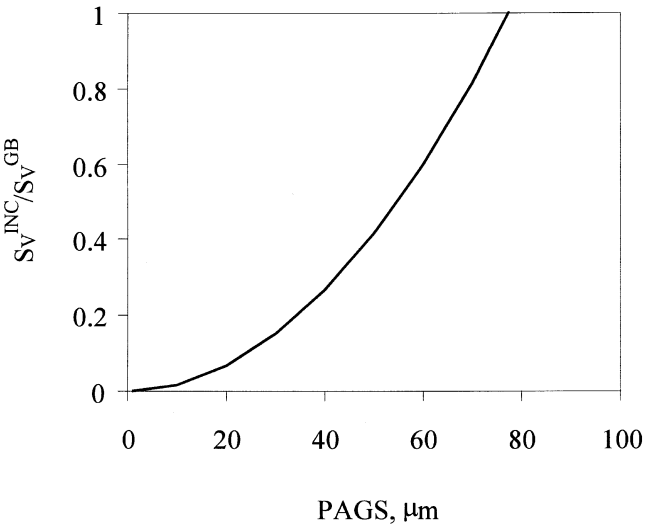

Fig. 5—Relationship between intragranular and grain boundary nucleation of ferrite as a function of the PAGS.

Therefore, S_V^{INC} can be calculated as follows:

$$S_V^{\text{INC}} = \frac{6}{d_3}\frac{d_\gamma}{(d_1 + d_2)/2} V_V = \frac{12 d_\gamma}{d_3 (d_1 + d_2)} V_V \qquad [7]$$

On the other hand, the intragranular nucleation sites per unit volume N_V^{INC} could be expressed by

$$N_V^{\text{INC}} = n_i S_V^{\text{INC}} \qquad [8]$$

where n_i is the number of nucleation sites per unit surface area of inclusion, which can be expressed as K^*/δ^2 where K^* is a constant and δ is the atomic spacing ($\delta = 2.5 \times 10^{-10}$ m).[23] After combining Eqs. [2] and [8], it could be concluded that $S_V^{\text{INC}}/S_V^{GB}$ represents a ratio between the density of intragranular and grain-boundary nucleation sites. Figure 5 shows the evolution of this ratio with PAGS. According to this figure, the intragranular nucleation of ferrite becomes more relevant as PAGS increases. For a PAGS of 76 μm, about 85 pct of the total number of nucleation sites for ferrite are intragranular, whereas for a PAGS of 11 μm, fewer than 1 pct of all the nucleation sites contribute to the intragranular nucleation of ferrite.

The equilibrium (or maximum) volume fraction of idiomorphic ferrite (V_{EQ}) formed during the isothermal decomposition of austenite at a given temperature was determined by a combination of dilatometric and metallographic analysis. When the dilatometric curve reaches the saturation, *i.e.*, no further dilatation due to transformation is observed, the isothermal decomposition of austenite is completed: the time this takes approximately represents the minimum holding time needed to reach the equilibrium volume fraction of idiomorphic ferrite. Since dilatometric curves do not allow us to discriminate between allotriomorphic and idiomorphic ferrite formation, only the metallographic examination of the microstructure will enable us to determine accurately V_{EQ}. Figure 6 shows the microstructures obtained after the isothermal decomposition of austenite over 1 h at 913 K for PAGSs of 11 and 76 μm. The experimental V_{EQ} values for idiomorphic ferrite obtained at that temperature (2 pct for a PAGS of 11 μm and 8 pct for a PAGS of 76 μm) are consistent with the fact that the intragranular nucleation of ferrite becomes more favorable than grain boundary nucleation as PAGS increases.

C. *Transformation Model*

Under a parabolic law, idiomorphic ferrite is considered to grow with time, the assumption of a semi-infinite extent

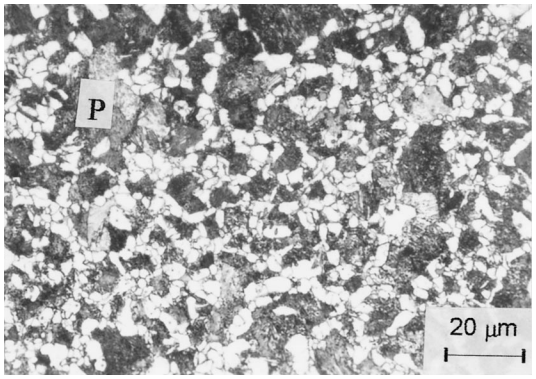

(*a*)

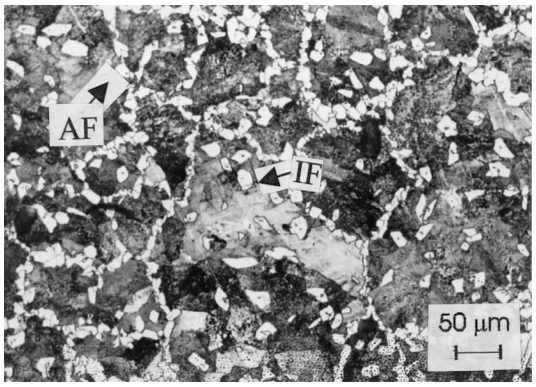

(*b*)

Fig. 6—Microstructures obtained after isothermal heat treatment at 913 K during 1 h for a PAGS of (*a*) 11 μm and (*b*) 76 μm. (IF is idiomorphic ferrite; AF is allotriomorphic ferrite; and P is pearlite.)

austenite with constant boundary conditions is considered a sensible approach for the kinetics of the isothermal decomposition of austenite into idiomorphic ferrite. On the other hand, the consideration of *paraequilibrium* is a good assumption for the kinetics of this transformation. In that case, substitutional solute atoms do not partition and the adjoining phases have identical *X*/Fe atom ratios, where *X* represents the substitutional solute elements. Then, the substitutional lattice is configurationally frozen, but interstitial solutes such as carbon are able to partition and attain equilibration of chemical potential in both phases.[11] The three-dimensional parabolic thickening constant (α_3) is given by[24]

$$\alpha_3 = \left[\frac{2D(\bar{x} - x^{\gamma\alpha})}{x^{\alpha\gamma} - \bar{x}}\right]^{1/2} \quad [9]$$

where $x^{\gamma\alpha}$ and $x^{\alpha\gamma}$ are the austenite and ferrite paraequilibrium carbon content at the interface, respectively, $\bar{x}$ is the average carbon content of the austenite, and *D* is the average diffusivity of carbon in austenite.

Idiomorphic ferrite formation occurs as follows: idiomorphs nucleate on inclusions randomly distributed in an existing austenite phase at a constant nucleation rate per unit area (*I*) and subsequently grow isotropically to form spherical particles. In diffusion-controlled growth, the radius of a particle formed after an incubation period (τ) will vary with the square root of time (*t*) as follows:

$$r = \alpha_3 (t - \tau)^{1/2} \quad [10]$$

where α_3 is considered constant as long as the far-field concentration in the matrix does not change. Therefore, the volume of an idiomorph after a time *t* is given by

$$\nu = \begin{cases} \frac{4\pi}{3} \alpha_3^3 (t - \tau)^{3/2}, & (t > \tau) \\ 0, & (t \leq \tau) \end{cases} \quad [11]$$

Moreover, the number of idiomorphs (*N*) formed in a time $d\tau$ is

$$N = IS_V^{INC} V d\tau \quad [12]$$

where *V* is the volume of austenite before isothermal decomposition.

At the stages of transformation, when particles start to impinge, the theory just described does not adequately describe the kinetics of idiomorphic ferrite formation. Avrami[25] introduced the concept of an *extended volume* to describe the volume of the particles whose growth is not impeded by impingement between particles. Particles are allowed to overlap and grow through each other. New nuclei forming in regions already transformed into idiomorphic ferrite, dubbed *phantom nuclei*, are also included in the extended volume calculation. Thus, the contribution of all the particles nucleated in the interval between τ and $\tau + d\tau$ to the extended volume of idiomorphic ferrite (V_{IDI}^e) can be expressed as

$$dV_{IDI}^e = \nu N = \frac{4\pi}{3} \alpha_3^3 (t - \tau)^{3/2} IS_V^{INC} V d\tau \quad [13]$$

However, the *actual* change in volume, dV_{IDI}, can be determined from the change in *extended volume* by just including the probability that some transformation to idiomorphic ferrite has already occurred. Thus, the volume of idiomorphic ferrite formed (V_{IDI}) could be written as

$$dV_{IDI} = \left(1 - \frac{V_{IDI}}{V}\right) dV_{IDI}^e \quad [14]$$

Separating variables and integrating Eq. [14], the following expression is obtained:

$$-ln\left(1 - \frac{V_{IDI}}{V}\right) = \frac{4\pi}{3} \int_0^t IS_V^{INC} \alpha_3^3 (t - \tau)^{3/2} d\tau \quad [15]$$

Finally, the volume fraction of idiomorphic ferrite ξ can be easily evaluated if it is assumed that *I* and α_3 are constant with time and that V_{EQ} is the maximum volume fraction of austenite that transforms to idiomorphic ferrite

$$\xi = \frac{V_{IDI}}{V} = V_{EQ}\left[1 - \exp\left(-\frac{8\pi}{15} IS_V^{INC} \alpha_3^3 t^{5/2}\right)\right] \quad [16]$$

The nucleation rate *I* has been calculated according to Lange *et al.*[26] and Reed and Bhadeshia,[27] taking into account the chemical composition of the studied steel; its value for a temperature of 913 K is 5.50×10^8 m^{-2} s^{-1}. The paraequilibrium carbon concentrations at the interface $x^{\alpha\gamma}$, $x^{\gamma\alpha}$ have been obtained using a calculated multicomponent phase diagram as reported by Shiflet *et al.*[28] The average diffusivity of carbon in austenite *D* has been calculated according to Bhadeshia.[29] Finally, S_v^{INC} has been calculated from Eq. [3]. All these values are listed in Table IV.

Table IV. S_V^{INC}, D, $x^{\alpha\gamma}$, $x^{\gamma\alpha}$, and α_3 Values for a Temperature of 913 K

S_V^{INC}, m^{-1}					
PAGS = 11 μm	PAGS = 76 μm	D, $m^2\ s^{-1}$	$x^{\alpha\gamma}$, wt pct	$x^{\gamma\alpha}$, wt pct	α_3, $m\ s^{-1/2}$
10.9×10^3	75.8×10^3	1.20×10^{-13}	0.016	0.903	6.01×10^{-7}

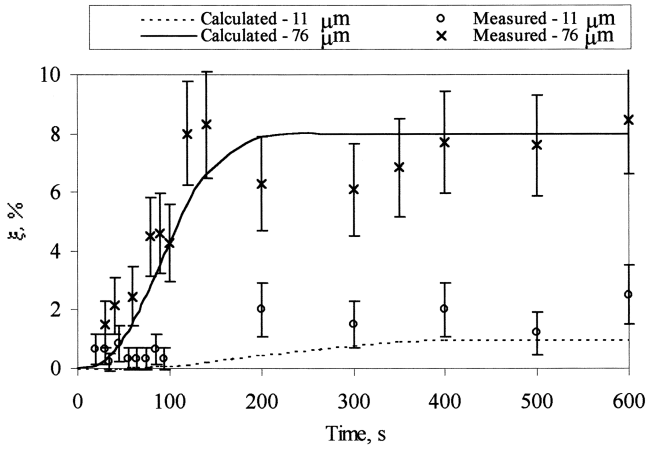

Fig. 7—Evolution of the volume fraction of idiomorphic ferrite, ξ, during the isothermal decomposition of austenite at 913 K, for two different PAGSs.

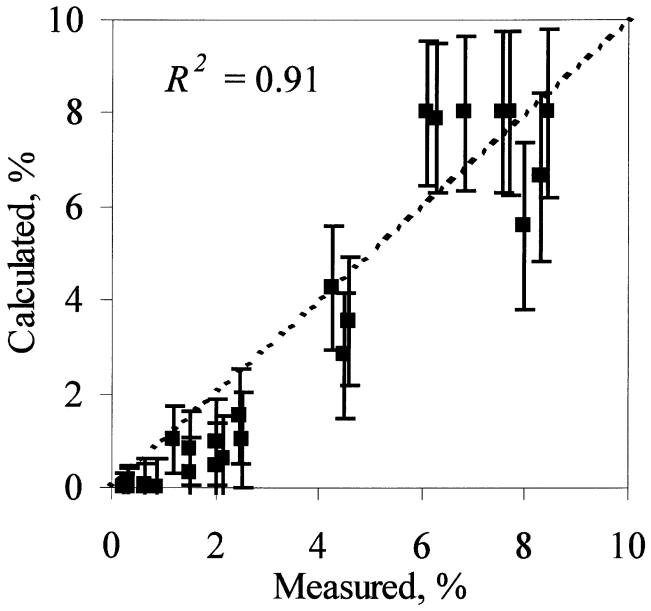

Fig. 8—A comparison of the experimental and calculated values of volume fraction of idiomorphic ferrite.

Figure 7 shows the evolution of the volume fraction of idiomorphic ferrite ξ formed during the isothermal decomposition of austenite at 913 K for two very different PAGSs. Figure 8 represents a comparison between the experimental and calculated values of ξ. The factor R^2 in this figure is the square correlation factor of the experimental and calculated volume fraction of idiomorphic ferrite. This parameter quantifies the accuracy of the model. Points lying on the line of unit slope show a perfect agreement between experimental and calculated values. From these figures it is concluded that a good agreement exists between experiment and theory.

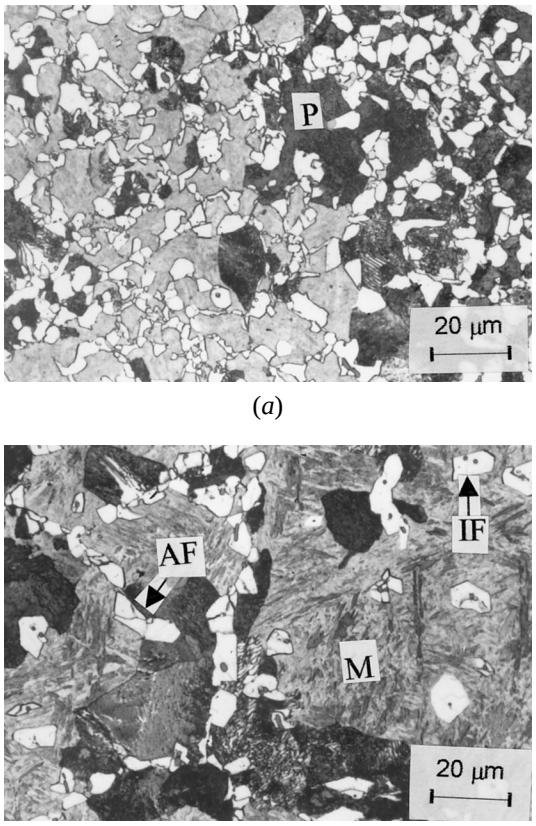

Fig. 9—Microstructures obtained after isothermal heat treatment at 913 K during 80 s for PAGSs of (*a*) 11 μm and (*b*) 76 μm. (IF is idiomorphic ferrite; AF is allotriomorphic ferrite; P is pearlite; and M is martensite.)

The accuracy of the model is higher than 90 pct, which can be considered excellent for kinetic models.

Additionally, the results in Figure 7 show a strong influence of the PAGS on the idiomorphic ferrite formation. As mentioned earlier, this influence is a consequence of the competition process between grain boundary and intragranular nucleation. As the PAGS increases, the number of intragranular nucleation sites increases to the detriment of the number of grain boundary nucleation sites. Consequently, the volume fraction of idiomorphic ferrite increases, as is shown in the micrographs in Figure 9.

IV. CONCLUSIONS

1. A kinetic model has been proposed for the isothermal formation of idiomorphic ferrite. The consideration of a parabolic law for the growth of idiomorphic ferrite is the most suitable representation of the idiomorphic ferrite formation kinetics. Experimental validation of this model has been carried out using dilatometric and metallographic analysis. An excellent agreement (with accuracy

higher than 90 pct in square correlation factor) has been found between the experimental and calculated volume fraction of idiomorphic ferrite isothermal formed at 913 K in a 0.37C-1.45Mn-0.11V (in wt. pct) microalloyed steel with two very different PAGSs.

2. In this steel, idiomorphic ferrite nucleates intragranularly on ellipsoidal manganese sulfide inclusions homogeneously distributed inside the austenite grains. Because of the excellent agreement between experimental and calculated results, it is concluded that the equation reported by Kluken and Grong,[18] which converts the analytical oxygen and sulfur concentration into an equivalent inclusion volume, is a sensible expression for the calculation of the volume fraction of inclusions in the steel.
3. An expression to determine the density of intragranular nucleation sites as a function of the PAGS, dimensions, and volume fraction of inclusion has been proposed. Since allotriomorphic and idiomorphic ferrite transformations are competitive processes, idiomorphic ferrite is formed instead of allotriomorphic ferrite, because the density of intragranular nucleation sites is in the order of that of the grain boundary nucleation sites. Thus, as the PAGS increases, idiomorphic ferrite formation is promoted.

ACKNOWLEDGMENTS

The authors acknowledge the financial support from the Spanish Comisión Interministerial de Ciencia y Tecnología (CICYT) (Project-PETRI No. 95-0089-OP). GSB Acero S.A and CEIT are thanked for providing the steel and for their collaboration in this project.

REFERENCES

1. F. Ishikawa, T. Takahashi, and T. Ochi: *Metall. Mater. Trans. A*, 1994, vol. 25A, pp. 929-36.
2. D.J. Abson and R.J. Pargerter: *Int. Met. Rev.*, 1986, vol. 31, pp. 141-94.
3. R.A. Farrar and P.L. Harrison: *J. Mater. Sci.*, 1987, vol. 22, pp. 3812-20.
4. Z. Zhang and R.A. Farrar: *Mater. Sci. Technol.*, 1996, vol. 12, pp. 237-60.
5. I. Madariaga and I. Gutiérrez: *Proc. Congreso Nacional de Tratamientos Térmicos y de Superficie TRATERMAT 98*, M. Carsí, F. Penalba, O.A. Ruano, and B.J. Fernández, CENIM-CSIC, Madrid, 1998, pp. 143-51.
6. C. García de Andrés, C. Capdevila, and F.G. Caballero: *Proc. Int. Conf. on Materials in Oceanic Environment EUROMAT 98*, L. Faria, ed. SPM-FEMS, Lisbon, Portugal, 1998, pp. 217-21.
7. I. Madariaga and I. Gutiérrez: *Acta Mater.*, 1997, vol. 37, pp. 1185-92.
8. I. Madariaga, I. Gutiérrez, C. García de Andrés, and C. Capdevila: *Scripta Mater.*, 1999, vol. 41, pp. 229-35.
9. K. Yamamoto, S. Matsuda, T. Haze, R. Chijiiwa, and H. Mimura: *Proc. Symp. on Residual and Unspecified Elements in Steel*, ASTM, Philadelphia, PA, 1989, pp. 1-24.
10. T. Ochi, T. Takahashi, and H. Harada: *Iron Steelmaker*, 1989, vol. 16, pp. 21-29.
11. H.K.D.H. Bhadeshia: *Progr. Mater. Sci.*, 1985, vol. 29, pp. 321-86.
12. C. García de Andrés, C. Capdevila, F.G. Caballero, and H.K.D.H. Bhadeshia: *Scripta Mater.*, 1998, vol. 39, pp. 853-56.
13. C. García de Andrés, F.G. Caballero, C. Capdevila, and H.K.D.H. Bhadeshia: *Scripta Mater.*, 1998, vol. 39, pp. 791-96.
14. F.G. Caballero, C. Capdevila, and C. García de Andrés: *Scripta Mater.*, 2000, vol. 42, pp. 1159-65.
15. H.K.D.H. Bhadeshia: *Bainite in Steels*, The Institute of Materials, London, 1992, p. 245.
16. C. García de Andrés, G. Caruana, and L.F. Alvarez: *Mater. Sci. Eng.*, 1998, vol. A241, pp. 211-15.
17. Vander Voort GF: *Metallography. Principles and Practice*, McGraw-Hill Book Company, New York, NY, 1984, p. 427.
18. A.O. Kluken and O. Grong: *Metall. Mater. Trans. A*, 1989, vol. 20A, pp. 1335-49.
19. S.M. Hodson: *MTDATA-Metallurgical and Thermomechanical Databank*, National Physical Laboratory, Teddington, United Kingdom, 1989, p. 1.
20. H.I. Aaronson: in *The Decomposition of Austenite by Diffusional Processes*, V.F. Zackay and H.I. Aaronson, eds. Interscience Publishers, New York, NY, 1962, pp. 387-546.
21. C.A. Dube, H.I. Aaronson, and R.F. Mehl: *Rev. Metall.*, 1958, vol. 3, pp. 201-13.
22. O. Grong: in *Metallurgical Modelling of Welding*, H.K.D.H. Bhadeshia, ed., Institute of Materials, London, 1997, p. 415.
23. J.W. Christian: *Theory of Transformations in Metals and Alloys*, 2nd ed., Pergamon Press, Oxford, United Kingdom, 1975, Part I, p. 476.
24. S.J. Jones and H.K.D.H. Bhadeshia: *Metall. Mater. Trans. A*, 1997, vol. 28A, pp. 2005-13.
25. M. Avrami: *J. Chem. Phys.*, 1939, vol. 7, pp. 1103-18.
26. W.F. Lange, M. Enomoto, and H.I. Aaronson: *Metall. Mater. Trans. A*, 1988, vol. 19A, pp. 427-40.
27. R.C. Reed and H.K.D.H. Bhadeshia: *Mater. Sci. Technol.*, 1992, vol. 8, pp. 421-35.
28. G.J. Shiflet, J.R. Bradley, and H.I. Aaronson: *Metall. Mater. Trans. A*, 1978, vol. 9A, pp. 999-1008.
29. H.K.D.H. Bhadeshia: *Met. Sci.*, 1981, vol. 15, pp. 477-79.